

Supporting Information

Enhanced Biofilm Penetration for Microbial Control by Polyvalent Phages Conjugated with Magnetic Colloidal Nanoparticle Clusters (CNCs)

Ling-Li Li^{1*}, Pingfeng Yu^{2*}, Xifan Wang², Sheng-Song Yu¹, Jacques Mathieu², Han-Qing Yu¹,
and Pedro J. J. Alvarez^{2**}

¹Department of Chemistry, University of Science and Technology of China, Hefei 230026, China

²Department of Civil and Environmental Engineering, Rice University, Houston, Texas 77005, USA

**Corresponding author; E-mail: alvarez@rice.edu. Phone: (713) 348-5903.

*Joint first authors

The supplementary information includes:

Materials and Methods

Synthesis and modification of magnetic CNCs.

Sample calculations.

Figures

Fig. S1. Polyvalent phage PEL1 infected both *E. coli* C3000 and *P. aeruginosa* PA01.

Fig. S2. XRD patterns of synthesized magnetic materials.

Fig. S3. Plaque formation capability of PEL1-CS-Fe₃O₄.

Fig. S5. Lack of phage inactivation or bacterial inhibition by different CNCs.

Fig. S6. Fraction of phages remaining in the bulk solution 30 min after dosage.

Fig. S7. Migration of CNCs within biofilm disrupted the integrity of biofilm.

Tables

Table S1. Growth parameters of phage PEL1

Table S2. Host range of phage PEL1

Supplementary reference

Synthesis and modification of magnetic CNCs. All reagents used were analytical grade and available commercially. The DI water was obtained from a Milli-Q synthesis system (Millipore, Billerica, MA). The Fe₃O₄ CNCs were synthesized by a solvothermal reaction.¹ Sodium acetate (4.32 g) and FeCl₃·6H₂O (1.72 g) were dissolved in ethylene glycol (60 mL) under vigorous magnetic stirring. The obtained homogeneous yellow solution was transferred to a 100 mL Teflon-lined stainless-steel autoclave. After 8 h heating at 200°C, the products were washed with ethanol and DI water each for three times.

The Fe₃O₄@SiO₂ CNCs were prepared by a versatile solution sol-gel method.² An aqueous dispersion of the Fe₃O₄ particles (17.5 mL, 0.02 g/mL) was added into a pure ethanol (70 mL) and concentrated ammonia solution (1.25 mL, 28 wt %), followed by ultrasonic dispersion for 15 min at room temperature. Afterward, 1.0 mL of tetraethyl orthosilicate (TEOS) was added dropwise, and the reaction proceeded under continuous mechanical stirring overnight. The resultant core-shell Fe₃O₄@SiO₂ CNCs were separated and washed with ethanol six times.

Amino groups were introduced onto the surface of Fe₃O₄@SiO₂ CNCs by conventional sol-gel reaction with APTES as a modifying agent.³ Fe₃O₄@SiO₂ (20 mg) CNCs were dispersed in a mixed solvent of ethanol/DI water (25 mL, v/v=70/30). NH₄OH (50 μL) and (3-aminopropyl) triethoxysilane (APTES, 60 μL) were added under vigorous stirring. After 24 hours of reaction, the products (Fe₃O₄@SiO₂-NH₂ core-shell CNCs) were washed with ethanol and DI water, respectively, three times.

Carboxyl groups were then functionalized by chemical reaction between the amino groups and succinic anhydride. The Fe₃O₄@SiO₂-NH₂ core-shell CNCs obtained in the previous step were dispersed in N,N-dimethylformamide, followed by adding succinic anhydride (15 mg) to functionalize the CNC with adequate carboxyl groups. The reaction took place under vigorous

stirring overnight and the products ($\text{Fe}_3\text{O}_4@\text{SiO}_2\text{-COOH}$ core-shell CNCs) were washed.

Chitosan-coated Fe_3O_4 (CS- Fe_3O_4) CNCs were synthesized via a versatile solvothermal reaction to obtain magnetic CNCs with porosity and high protonation of amino group.⁴ Typically, $\text{FeCl}_3 \cdot 6\text{H}_2\text{O}$ (1.50 g), NaOAc (3.6 g), chitosan (0.5 g), and PVP (1.0 g) were added into ethylene glycol (70 mL) to obtain a transparent solution under vigorous stirring. This mixture was then transferred to a 100 mL Teflon-lined stainless-steel autoclave for heating at 200°C for 8 h. The products were collected and washed exhaustively to remove the free chitosan.

Sample calculations. Phage immobilized onto CNCs (PFU/mg) = [Initial phage amount (PFU/mL) – Phage inactivated by EDC and NHS (PFU/mL) – Phage inactivated by CNCs (PFU/mL) – Total residual free phages amount (PFU/mL)] ÷ Total CNCs (mg/mL). The phages amounts were quantified in triplicate by double-layer plaque assay using mixed bacteria ($\text{OD}_{600} = 0.5$, equal ratio of *P. aeruginosa* and *E. coli*).

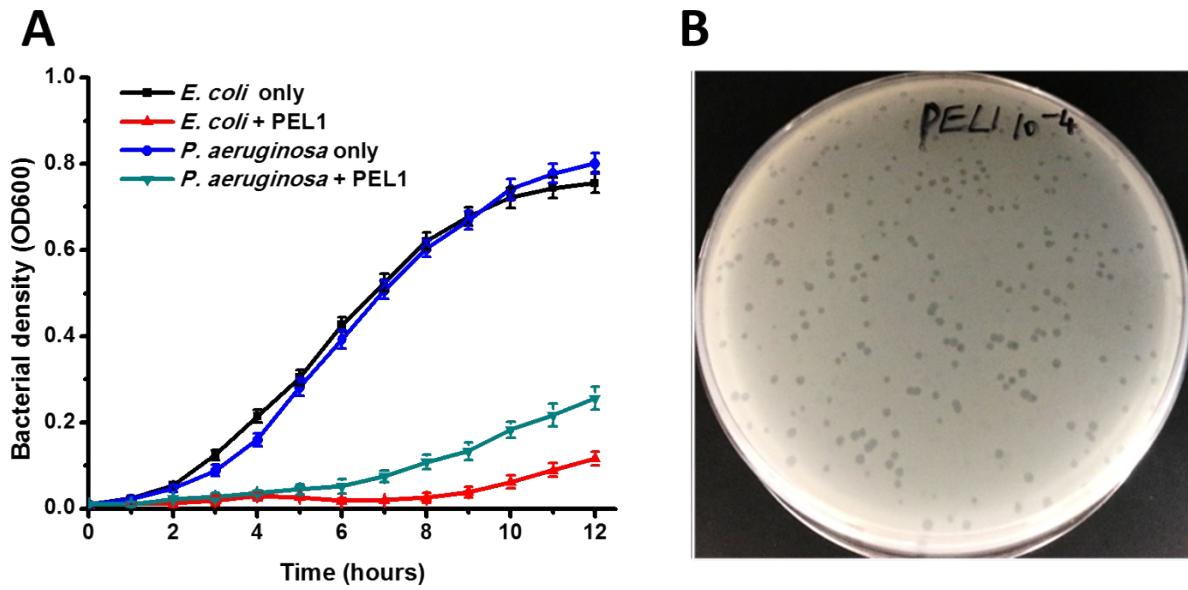


Fig. S1. Polyvalent phage PEL1 infected both *E. coli* C3000 and *P. aeruginosa* PA01. Phage PEL1 inhibited the growth of each bacterium during batch growth experiments at MOI of 10 (A), and formed clear plaques in the soft agar inoculated with both bacteria (B). Error bars indicate \pm one standard deviation from the mean of triplicate independent experiments.

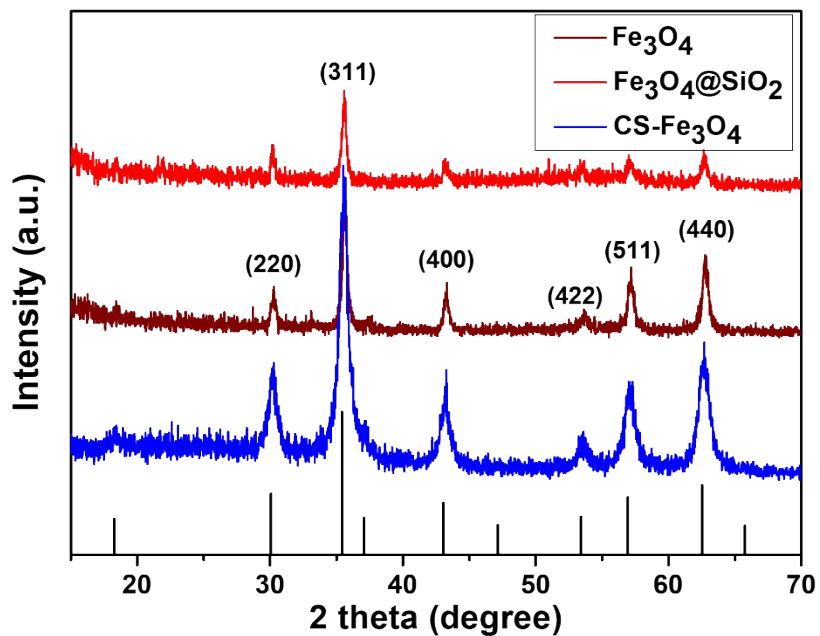


Fig. S2. XRD patterns of synthesized magnetic materials. JCPDS card NO. 65-3107 (black, Fe_3O_4 , magnetite).

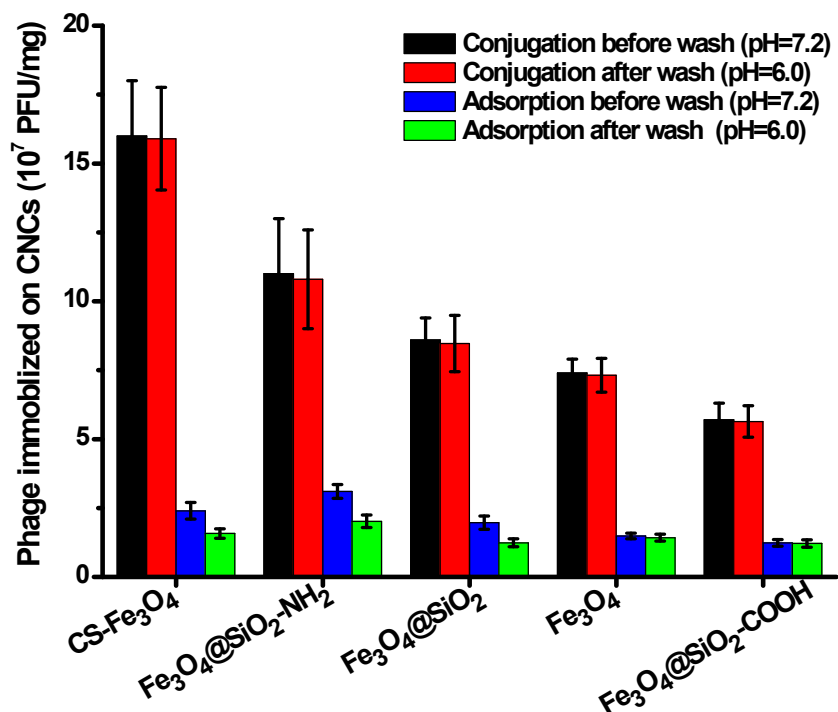


Fig. S3. **Phage PEL1 immobilized on CNCs due to conjugation and non-specific attachment.**

The number of phages immobilized onto CNCs by covalent bonds (i.e., conjugation) or adsorption was quantified by double-layer plaque assay as the difference between the initial phage amount and the total number of free phages remaining in the conjugation plus washing solutions. For estimating adsorption, EDC and NHS were omitted to avoid stimulating conjugation. During the washing step (repeated three times), PEL1-CNC complexes were vortexed at 240 rpm for 10 seconds and precipitated under magnetic field to detach loosely bound phages. Error bars indicate \pm one standard deviation from the mean of triplicate independent experiments.

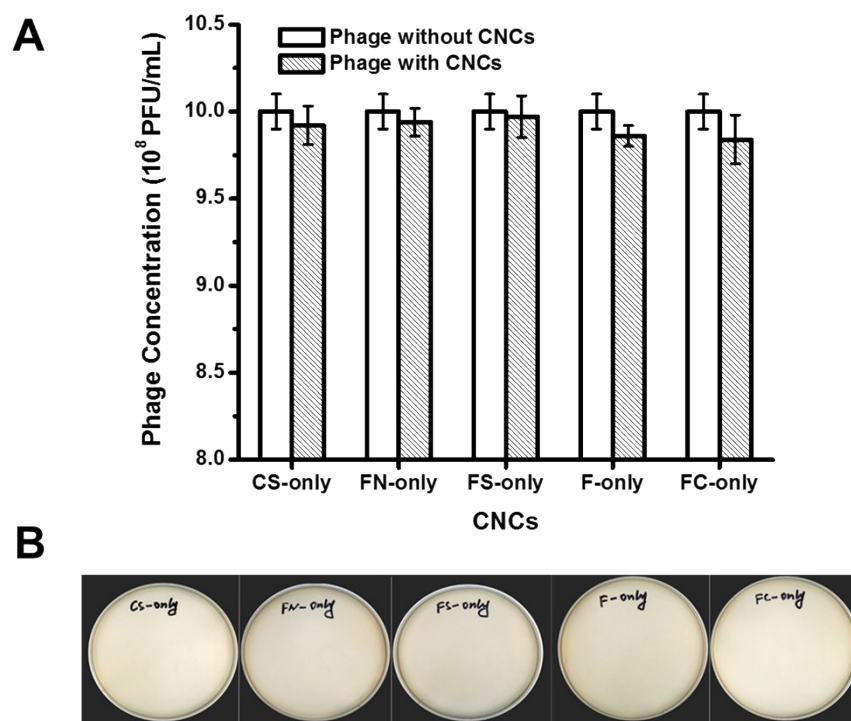


Fig. S4. Lack of phage inactivation (A) or bacterial inhibition (B) by different CNCs. Panel A shows that these CNCs exerted little toxicity towards phage PEL1 since the sum of PFUs from free phages in bulk solution and attached phage on CNCs has no statistical difference with the PFUs in initial phage solution. Panel B shows no significant inhibitory effect on bacterial lawns (i.e., *E. coli* C3000 plus *P. aeruginosa* PA01) by CS-Fe₃O₄ (CS-only), Fe₃O₄@SiO₂ core-shell CNCs (FS-only), Fe₃O₄@SiO₂-NH₂ CNCs (FN-only), Fe₃O₄ CNCs (F-only) or Fe₃O₄@SiO₂-COOH CNCs (FC-only). Error bars indicate \pm one standard deviation from the mean of triplicate independent experiments.

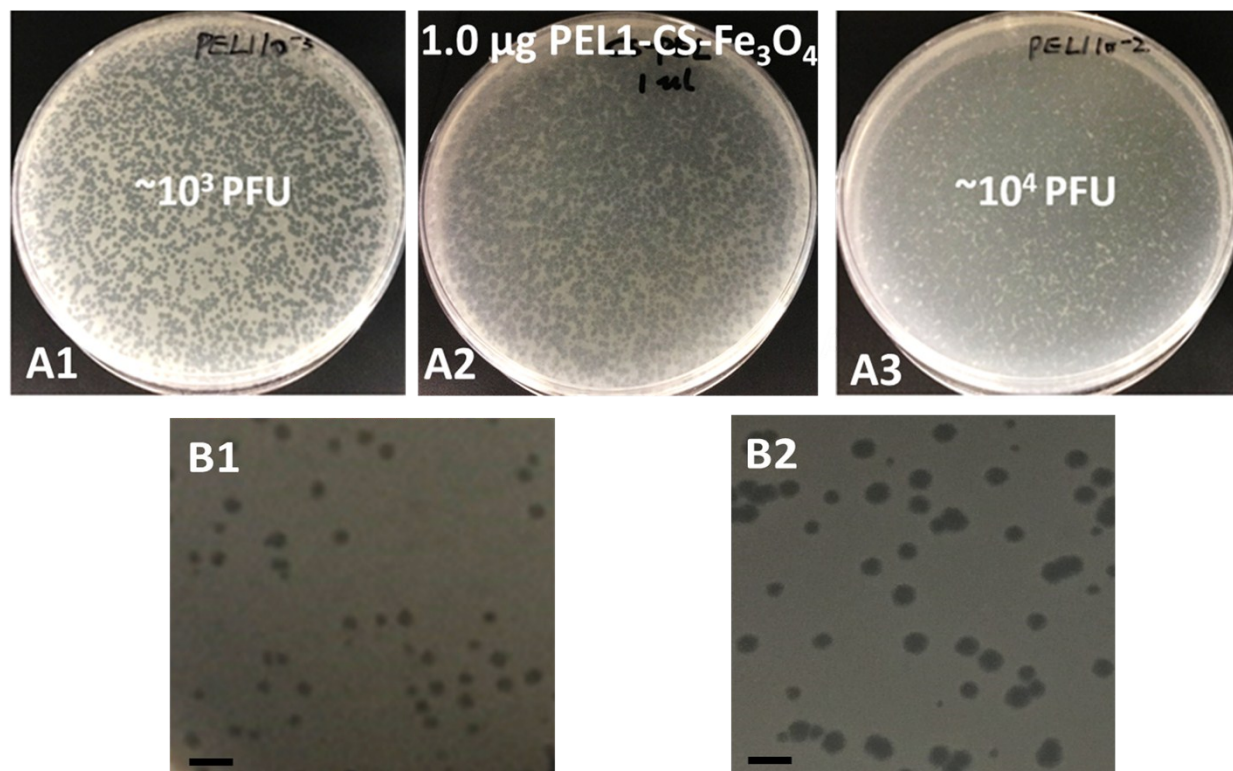


Fig. S5. **Plaque formation capability of PEL1-CS-Fe₃O₄.** Panel A1, A2 and A3 showed the plaque formation capability of 10³ PFU of free phage, 1.0 μg PEL1-CS-Fe₃O₄, and 10⁴ PFU of free phage, respectively. Panel B1 and B2 showed the plaque morphology from free phages and PEL1-CS-Fe₃O₄ complexes, respectively. The plaque formation capability of 1.0 μg PEL1-CS-Fe₃O₄ lay between 10³-10⁴ PFU free phage. Further serial dilution and plating showed that 1.0 μg PEL1-CS-Fe₃O₄ corresponded to approximately $(5.2 \pm 0.7) \times 10^3$ centers of infection (COI) on the two-species bacterial lawn. Scale bar represents 10 mm.

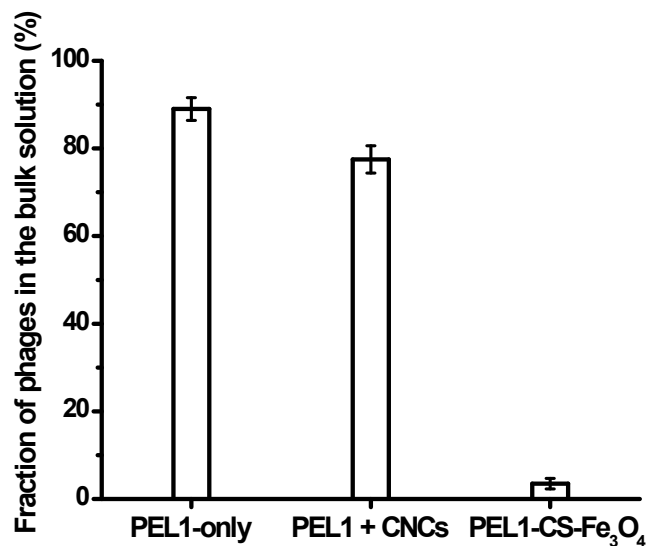


Fig. S6. **Fraction of phages remaining in the bulk solution 30 min after dosage.** Free phages (PEL1-only) are mainly dispersed in the bulk solution, while the conjugated phage (PEL1-CS-Fe₃O₄) effectively penetrate the biofilm under magnetic field. Combination of free phage and CNCs (PEL1 + CNCs) slightly enhanced the free phage dispersion. Error bars indicate \pm one standard deviation from the mean of triplicate independent experiments.

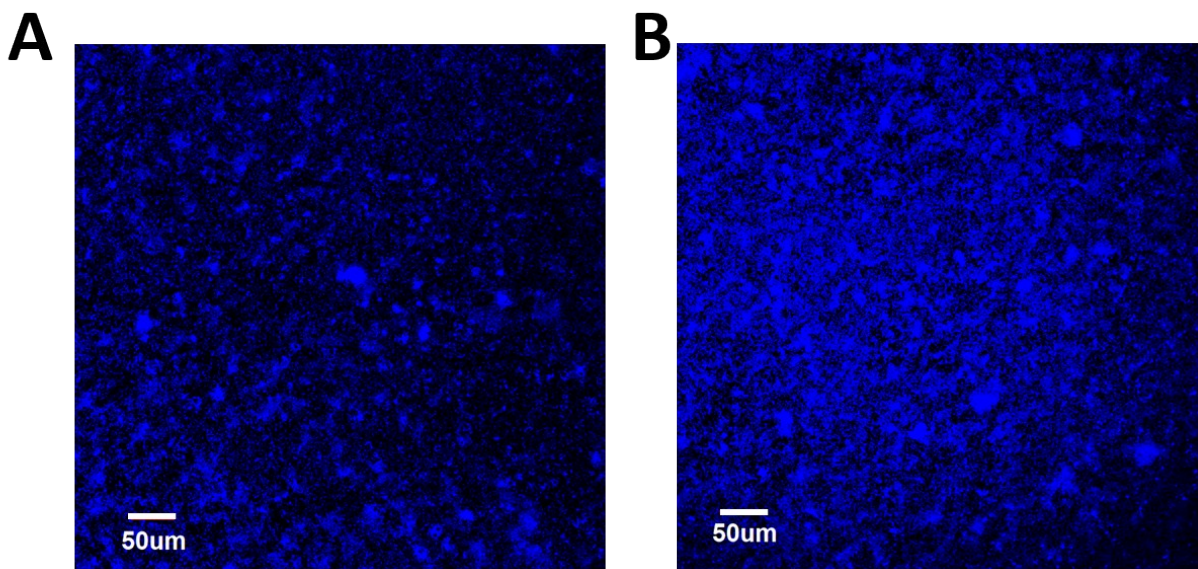


Fig. S7. **Migration of CNCs within biofilm disrupted the integrity of the biofilm.** Panel A shows disrupted biofilm due to horizontal migration of CNCs under magnetic field (660 gauss), and Panel B showed the intact biofilm without treatment by CNCs. Bacterial cells (live and dead) were stained with DAPI. Scale bar represents 50 μm .

Table S1. **Growth parameters of phage PEL1^a**

Host	Adsorption rate constant (10⁻¹⁰ mL/min)	Latent time (min)	Burst size (PFU/cell)
<i>P. aeruginosa</i> PA01	10.9	35	75±6
<i>E. coli</i> C3000	7.38	40	98±6

^a Data shown are the means of results from triplicate independent experiments in TSB medium supplemented with 10 mM Ca²⁺.

Table S2. Host range of phage PEL1

Bacteria	ATCC #	Family	Infectivity ^a
<i>E. coli</i> C3000	15597	Enterobacteriaceae	++
<i>E. coli</i> K-12	10798	Enterobacteriaceae	++
<i>E. coli</i> NDM-1	BAA-2452	Enterobacteriaceae	++
<i>Enterobacter cloacae</i>	13047	Enterobacteriaceae	--
<i>Klebsiella oxytoca</i>	700324	Enterobacteriaceae	--
<i>Salmonella typhimurium</i>	700720	Enterobacteriaceae	--
<i>Serratia marcescens</i>	133880	Enterobacteriaceae	--
<i>P. aeruginosa</i> PA01	15692	Pseudomonadaceae	++
<i>P. aeruginosa</i> HER1018	BAA-47	Pseudomonadaceae	++
<i>P. aeruginosa</i> Migula	700829	Pseudomonadaceae	++
<i>P. putida</i>	700007	Pseudomonadaceae	--
<i>P. syringae</i>	19310	Pseudomonadaceae	--
<i>P. fluorescens</i>	13525	Pseudomonadaceae	--
<i>P. putida</i> F1	700007	Pseudomonadaceae	--
<i>Bacillus subtilis</i>	6051	Bacillaceae	--
<i>Bacillus cereus</i>	10987	Bacillaceae	--

^a Spot tests and plaque assay showed infection (++) or no infection (--).

Supplementary References

1. Y. Tang, S. Liang, S. Yu, N. Gao, J. Zhang, H. Guo and Y. Wang, *Colloids and Surfaces A: Physicochemical and Engineering Aspects*, 2012, **406**, 61-67.
2. Y. Deng, Y. Cai, Z. Sun, J. Liu, C. Liu, J. Wei, W. Li, C. Liu, Y. Wang and D. Zhao, *Journal of the American Chemical Society*, 2010, **132**, 8466-8473.
3. H. Yang, L. Qin, Y. Wang, B. Zhang, Z. Liu, H. Ma, J. Lu, X. Huang, D. Shi and Z. Hu, *International Journal of Nanomedicine*, 2015, **10**, 77-88.
4. M. Shen, W. Jia, C. Lin, G. Fan, Y. Jin, X. Chen and G. Chen, *Nanoscale Research Letters*, 2014, **9**, 558-558.